Structural Changes in the Photoactive Site of Proteorhodopsin during the Primary Photoreaction†

Vladislav Bergo,‡ Jason J. Amsden,‡ Elena N. Spudich,§ John L. Spudich,§ and Kenneth J. Rothschild*,‡

Department of Physics, Molecular Biophysics Laboratory, Boston University, Boston, Massachusetts 02215, and Center for Membrane Biology, Department of Biochemistry and Molecular Biology, University of Texas Medical School, Houston, Texas 77030

Received December 7, 2003; Revised Manuscript Received April 29, 2004

ABSTRACT: Proteorhodopsin (PR), found in marine γ-proteobacteria, is a newly discovered light-driven proton pump similar to bacteriorhodopsin (BR). Because of the widespread distribution of proteobacteria in the worldwide oceanic waters, this pigment may contribute significantly to the global solar energy input in the biosphere. We examined structural changes that occur during the primary photoreaction (PR → K) of wild-type pigment and two mutants using low-temperature FTIR difference spectroscopy. Several vibrations detected in the 3500−3700 cm^{-1} region are assigned on the basis of $H_2O \rightarrow H_2{}^{18}O$ exchange to the perturbation of one or more internal water molecules. Substitution of the negatively charged Schiff base counterion, Asp97, with the neutral asparagine caused a downshift of the ethylenic (C═C) and Schiff base (C═N) stretching modes, in agreement with the 27 nm red shift of the visible λ_{max}. However, this replacement did not alter the normal all-*trans* to 13-*cis* isomerization of the chromophore or the environment of the detected water molecule(s). In contrast, substitution of Asn230, which is in a position to interact with the Schiff base, with Ala induces a 5 nm red shift of the visible λ_{max} and alters the PR chromophore structure, its isomerization to K, and the environment of the detected internal water molecules. The combination of FTIR and site-directed mutagenesis establishes that both Asp97 and Asn230 are perturbed during the primary phototransition. The environment of Asn230 is further altered during the thermal decay of K. These results suggest that significant differences exist in the conformational changes which occur in the photoactive sites of proteorhodopsin and bacteriorhodopsin during the primary photoreaction.

Proteorhodopsin (PR)[1] is a newly discovered member of the microbial rhodopsin family which functions as a light-driven proton pump in various species of marine γ-proteobacteria. Since the initial discovery of PR in the Pacific Ocean near the California coast (*2*), similar proteins have been found worldwide including Hawaii, Antarctica, and the Red Sea (*2*, *3*, *54*). Their widespread distribution plus the estimated concentration of PR in these organisms suggests that solar energy absorption by PR may constitute a significant fraction of the total solar energy conversion by the biosphere (*2*).

Like other microbial rhodopsins, proteorhodopsin contains an all-*trans*-retinylidene chromophore similar to the light-adapted form of bacteriorhodopsin (BR), a well-studied archaeal proton pump in *Halobacterium salinarum* (*4*). The photochemical reaction cycle of PR was previously studied by combined FTIR and UV−visible kinetic spectroscopy, and a model of the PR photocycle has been proposed (*5*, *6*), which exhibits many features of the BR photocycle. For example, like BR the absorption of light by PR results in the all-*trans*- → 13-*cis*-retinal isomerization and formation of a red-shifted K intermediate (*5*). The K intermediate thermally decays within several microseconds, producing the blue-shifted M intermediate. During the formation of M, a proton is transferred from the Schiff base to its primary counterion Asp97. In the subsequent M → N step, the Schiff base is reprotonated, presumably from Glu108 located on the cytoplasmic side of the protein. Recovery of the protein resting state occurs within ∼20 ms and involves reisomerization of the chromophore to the all-*trans* state.

Although PR was shown to exhibit an outwardly directed proton pumping similar to BR (*2*), some differences in the proton transport mechanism have emerged. Unlike BR, where proton release (∼40 μs) precedes proton uptake (*7*, *8*), in PR the proton release is significantly slowed (several milliseconds) and occurs after the proton uptake (*6*). This effect was attributed to the absence of two carboxylate groups, Glu194 and Glu204, that function as part of the proton release mechanism in BR (*6*). It has been suggested that, unlike BR, the efficient proton transport by PR may

† This study was supported by NIH Grant R01EY05499 to K.J.R., NIH Grant R37GM27750, Human Frontier Science Program Grant RGP38, and support from the Robert A. Welch foundation to J.L.S.

* To whom correspondence should be addressed. Tel: 617-353-2603. Fax: 617-353-5167. E-mail: kjr@bu.edu.

‡ Boston University.

§ University of Texas Medical School.

[1] Abbreviations: FTIR, Fourier transform infrared spectroscopy; PR, the unphotolyzed state of Monterey Bay surface proteorhodopsin (eBAC31A08, designated GPR in ref *1*); K, M, N, and O, spectrally distinct intermediates of the photochemical reaction cycle of microbial rhodopsins; BR, bacteriorhodopsin; NpSRII, sensory rhodopsin II of *Natronobacterium pharaonis*; SB, Schiff base; HOOP, hydrogen out of plane; OG, octyl glucoside.

10.1021/bi0361968 CCC: $27.50
Published on Web 06/24/2004

require a second photoexcitation (*5*). Although the 3-D structure of PR is not yet elucidated, comparison of the primary sequence of BR and PR also indicates that there may be differences in the structure of the active site surrounding the protonated Schiff base. For example, in BR there is a non-hydrogen-bonding alanine (Ala215) located on the G-helix just one residue below the lysine (Lys216), which forms the Schiff base linkage to the chromophore. In contrast, in PR there is a hydrogen-bonding asparagine (Asn230) below the corresponding lysine.

Fourier transform infrared (FTIR) difference spectroscopy has been successfully used to elucidate many of the details of the proton transport mechanism in BR (*9*−*13*) and more recently to study protein structural changes that occur in other microbial rhodopsins, such as sensory rhodopsin II (*14*−*16*) and *Neurospora* rhodopsin (*17*, *18*). In the case of proteorhodopsin, kinetic FTIR spectra were recorded in the millisecond time range, reflecting predominantly formation of the blue-shifted N-like intermediate (*5*, *6*). Although the early red-shifted K-like intermediate was observed in the microsecond time-resolved spectra (*5*), up to now there has been no detailed analysis by FTIR difference spectroscopy of this intermediate.

To further examine structural changes that occur during the early photocycle of proteorhodopsin, we used low-temperature static FTIR difference spectroscopy. This approach has the advantage that spectra above 1800 cm^{-1} can be recorded with high signal-to-noise ratio, allowing the detection of various X−H stretching vibrations, in particular the O−H stretching modes of internal water molecules. The difference spectra revealed formation of a red-shifted K-like photoproduct that was similar to the K intermediate of BR in the C═C and C−C chromophore stretching modes. However, unlike the K formed by BR, the early photoproduct of proteorhodopsin exhibited greater thermal stability as indicated by the very similar spectra recorded at 80 and 170 K. Several prominent bands have been assigned to structural changes of Asp97 and Asn230 on the basis of the substitutions Asp97 → Asn and Asn230 → Ala. Interestingly, water molecules which are identified to be involved in the PR → K transition as well as the overall chromophore isomerization are not affected by the Asp97 → Asn substitution. In contrast, the Asn230 → Ala substitution alters the structural changes of both water and the chromophore, suggesting that it plays an important role in the PR photoactive site.

MATERIALS AND METHODS

Protein Expression and Purification. All procedures for the site-directed mutagenesis, plasmid construction, and expression in the *Escherichia coli* UT5600 strain were identical to those described previously (*6*). The N230A mutant was constructed by PCR mutagenesis using the QuikChange site-directed mutagenesis kit (Stratagene). The oligonucleotide primers were 5′-CCTTGCTGACTTTGTTG-CCAAGATTCTATTTGGTTT-3′ and 5′-AAACCAAATA-GAATCTTGGCAACAAAGTCAGCAAGG-3′. The mutation was verified by DNA sequencing. After the induction period, the cells expressing His-tagged wild-type, D97N, or N230A PR were centrifuged at 1000*g*, resuspended in 5 mM $MgCl_2$ and 150 mM Tris-HCl, pH 7.0, incubated with 100 μg/mL lysozyme for 2 h at 4 °C ,and disrupted by sonication. Unbroken cells were removed by low-speed centrifugation. The membranes containing pigment were collected by centrifugation (39000*g*, 30 min) and solubilized in a wash buffer (50 mM KP_i, 300 mM NaCl, 5 mM imidazole, and 1.5% octyl glucoside (OG), pH 7.0) for at least 1 h at 4 °C. Unsolubilized membranes were removed by centrifugation at 28000*g* for 30 min. The supernatant was incubated with a His-binding resin on a shaker at 4 °C for at least 1 h. The bound resin was applied to a 10 cm chromatography column and washed with 3× volumes of wash buffer followed by elution buffer (50 mM KP_i, 300 mM NaCl, 250 mM imidazole, and 1.0% OG, pH 7.0). The sample purity was assessed by the UV−visible spectroscopy and SDS−PAGE analysis (*2*).

Proteoliposome Reconstitution. Purified His-tagged PR was reconstituted in the *E. coli* polar lipids (Avanti, Alabaster, AL) at 1:10 protein-to-lipid (w/w) ratio. Lipids initially dissolved in chloroform were dried under argon and resuspended in the dialysis buffer (50 mM potassium phosphate, 300 mM NaCl, pH 7.0) to which OG was added to the final concentration of 1%. The lipid solution was incubated with the OG-solubilized protein for 1 h on ice and dialyzed against the dialysis buffer with three buffer changes every 24 h. The reconstituted protein was centrifuged for 15 min and resuspended in the sample buffer (50 mM CHES, 150 mM NaCl, pH 9.5).

FTIR Difference Spectroscopy. The protein samples for the low-temperature FTIR measurements were prepared as previously reported (*15*) using approximately 200 μg of the protein for each experiment. The samples were deposited on CaF_2 windows and stored under argon. Difference spectra were recorded at 4 cm^{-1} resolution using a Bio-Rad FTS-60A FTIR spectrometer (Bio-Rad, Digilab Division, Cambridge, MA) equipped with a liquid nitrogen cooled MCT detector. A Dolan-Jenner (Woburn, MA) model 180 illuminator (150 W, tungsten−halogen) and a fiber-optic light guide were used for sample illumination in combination with the 500 nm short-pass and 570 nm long-pass optical filters (Corion Corp., Holliston, MA). Difference spectra were obtained at 80 and 170 K as previously described for bacteriorhodopsin (*19*). Photoreactions were also measured at 215 K using a single illumination of the protein dark state with yellow (475 nm long-pass) light for 4 min.

RESULTS

FTIR Difference Spectra of Wild-Type PR Recorded at 80 K. The PR → K difference spectrum was recorded using a protocol similar to earlier low-temperature FTIR difference measurements on BR (*10*, *19*, *20*). The PR sample was first cooled to near 80 K in the dark. It was then illuminated with a blue light ($415 < \lambda < 500$ nm), a spectrum was recorded in the dark and then illuminated with orange light ($800 > \lambda > 570$ nm), and a second spectrum was recorded in the dark. Several such cycles of blue and orange light were repeated and the difference spectra averaged in order to decrease the signal/noise ratio.

The resulting difference spectrum (Figure 1, top) closely resembles a single "first push" difference spectrum, where spectra were measured before and after only the first blue light illumination (data not shown). This indicates that, like

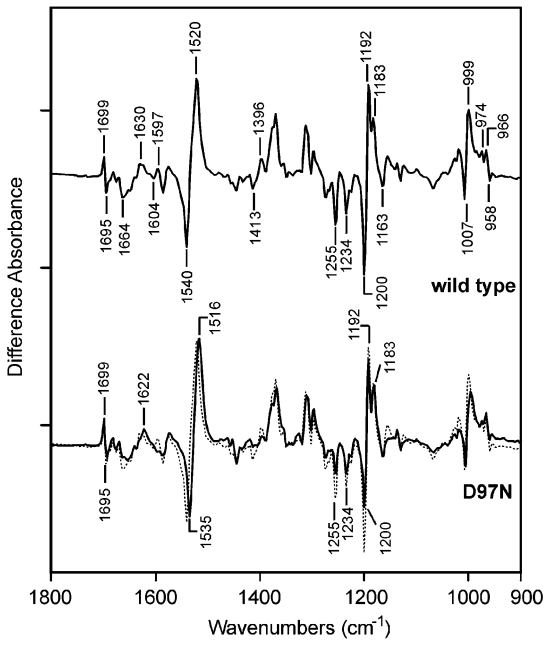

FIGURE 1: Comparison of FTIR difference spectra recorded at 80 K for proteorhodopsin wild type (top, solid line, and bottom, dotted line) and the D97N mutant (bottom, solid line) in the 900−1800 cm^{-1} spectral region. The spectra were recorded at 4 cm^{-1} spectral resolution. Each spectrum represents the average of at least 40 difference spectra, each consisting of 1000 individual scans. Spacing of *Y*-axis (difference absorbance) markers corresponds to 1×10^{-4} OD.

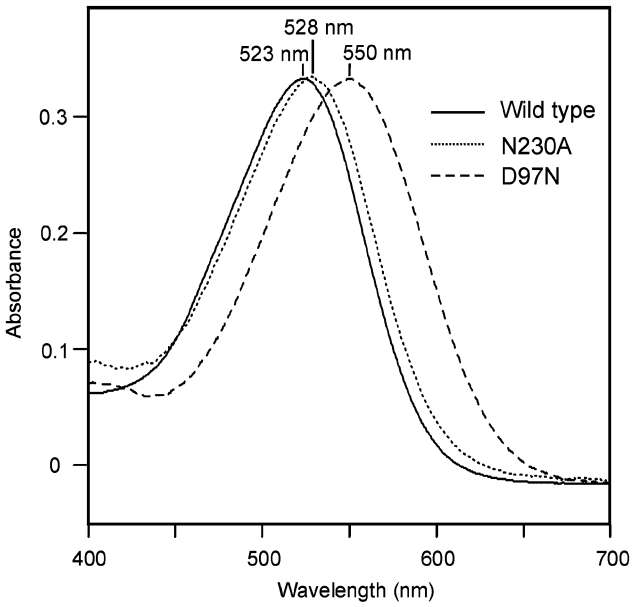

FIGURE 2: Visible absorption spectra of the wild-type PR and mutants D97N and N230A measured in the sample buffer (pH 9.5) in the presence of 1% octyl glucoside.

BR and many vertebrate rhodopsins (*21*−*24*), blue light converts the resting state of PR to a K-like red-shifted photointermediate, while orange light (above 570 nm) photoreverses the reaction. Very similar difference spectra were also obtained when the sample was illuminated at room temperature prior to cooling (data not shown), indicating that spectral differences between the light- and dark-adapted forms of PR are small. A similar conclusion was also reached on the basis of FT Raman studies of PR (*6*). The K intermediate in PR also exhibited unusual temperature stability since there are only small changes in intensity observed between the PR to K difference spectra recorded at 80 and 170 K as discussed later.

Overall, the FTIR difference spectrum of the PR → K transition indicates that, like BR, the initial photochemistry involves an all-*trans* to 13-*cis* isomerization of the chromophore. The PR difference spectrum exhibits a pair of strong negative/positive bands in the ethylenic stretching region at 1540 cm^{-1} (−) and 1520 cm^{-1} (+) similar to difference bands found in the BR → K spectrum at 1530 and 1515 cm^{-1} (*10*, *19*, *20*, *25*). The negative 1540 cm^{-1} band, which is close to the peak found at 1535 cm^{-1} in the FT Raman (*6*) and at 1533 cm^{-1} in resonance Raman spectra (*4*), arises from retinal ethylenic C═C stretching vibrations of the PR dark-adapted state. Correspondingly, the positive 1520 cm^{-1} band arises from the C═C stretching mode of the K photointermediate. The higher frequency of the negative band at 1540 cm^{-1} compared to the Raman spectra is most likely due to overlap with the positive band at 1520 cm^{-1}, which causes a "splitting" effect. An empirical inverse relationship between the visible absorption maximum and the ethylenic stretching frequency has been established for rhodopsin (*26*) and discussed recently in terms of microbial rhodopsins (*17*, *27*). This correlation predicts an approximately 5 nm red shift in λ_{max} for each 1 cm^{-1} decrease of the C═C stretching frequency. Therefore, the 15−20 cm^{-1} downshift between the unphotolyzed state of wild-type PR with a λ_{max} near 523 nm (Figure 2, top) and its photointermediate may indicate a slightly larger red shift in the visible absorption, compared to the 60 nm spectral shift between BR_{570} and K_{630} at low temperature. The previously reported time-resolved PR → K difference spectrum reveals a different set of C═C stretching bands consisting of two negative bands at 1540 and 1529 cm^{-1} and a positive band at 1514 cm^{-1} (*5*). As noted by Friedrich et al. (*5*) the negative 1529 cm^{-1} band is most likely due to the low-pH form of PR. In addition, the lower frequency of the reported positive band at 1514 cm^{-1} (*5*) compared to the 1520 cm^{-1} band observed in the current study may be caused by overlap of this negative 1529 cm^{-1} band.

Prominent negative bands are also found in the retinal fingerprint region at 1255, 1200, and 1163 cm^{-1}, close to the peaks at 1255, 1203, and 1170 cm^{-1} assigned to various C−C stretching modes of the all-*trans*-retinal chromophore in the BR → K difference spectrum (*25*) on the basis of resonance Raman spectroscopy and isotope labeling (*28*). Similar bands also appear in the resonance Raman spectrum of PR at 1255, 1198, and 1169 cm^{-1} (*4*). A strong positive band at 1192 cm^{-1} is likely to arise from the mixed C14−C15 and C10−C11 stretching vibration of the 13-*cis*-retinal chromophore, which appears at 1194 cm^{-1} in BR (*25*).

Despite the overall similarity between the BR and PR assigned chromophore bands, several spectral differences are evident. A negative band near 1216 cm^{-1} assigned to the C8−C9 stretching mode in BR (*28*) is not found in the PR spectrum, in agreement with the resonance Raman data (*4*), while a new negative band appears at 1234 cm^{-1}. A new positive band also appears near 1183 cm^{-1} in PR, which might arise from photoexcitation of a 13-*cis* chromophore that is found in both light- and dark-adapted forms of PR (*5*). However, the PR → K spectrum does not exhibit a

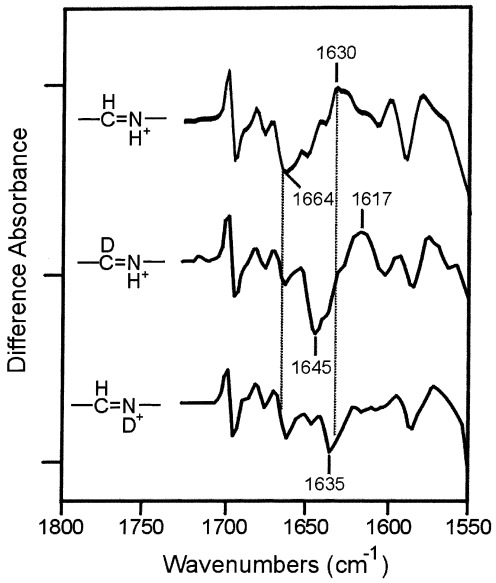

FIGURE 3: FTIR difference spectra recorded at 80 K and 4 cm^{-1} resolution for wild-type PR containing unlabeled chromophore (top), hydrogen at the retinal C15 position substituted with deuterium (middle), and hydrogen at the Schiff base nitrogen substituted with deuterium (bottom). Isotope labeling at the C15 position was achieved by growing *E. coli* cells on a medium supplemented with the C15D retinal instead of the normal retinal. Isotope labeling at the SB was achieved by the hydrogen−deuterium solvent exchange as described before (*15*).

negative band near 1347 cm^{-1}, which is indicative of contribution from the 13-*cis* photocycle (*29*, *30*). A strong pair of bands appear at 1007/999 (−/+) cm^{-1}, most likely due to a shift in frequency of the methyl rock vibration found in the resonance Raman spectrum at 1006 cm^{-1} (*4*). Significant differences are also found in the hydrogen out-of-plane (HOOP) mode regions of PR and BR (900−1000 cm^{-1}), which are sensitive to nonplanar distortions of the retinal (*31*, *32*). In particular, positive peaks appear at 974 and 966 cm^{-1} in contrast to a strong band near 956 cm^{-1} (+) assigned to the C15H HOOP mode in the K intermediate of BR (*33*). A small band found at 958 cm^{-1} (−) is also present in the resonance Raman spectrum (*4*) and most likely arises from the HOOP mode of the dark state PR.

In the amide I region (1600−1700 cm^{-1}), peaks appear near 1699 (+), 1695 (−), 1664 (−), and 1630 (+) cm^{-1}. The weak intensity of these bands indicates that only limited changes occur in the protein structure during the early photocycle, similar to BR (*34*). The absence of strong protein vibrations in this region allowed us to identify difference bands arising from the Schiff base C═N stretching mode on the basis of H/D exchange and isotope labeling of the chromophore (Figure 3). Single deuteration at the retinal C15 position downshifts most of the negative peak near 1664 cm^{-1} to 1645 cm^{-1} and shifts a positive 1630 cm^{-1} band with a possible component near 1624 cm^{-1} to 1617 cm^{-1} (middle trace). The 1664 cm^{-1} band is further downshifted to 1635 cm^{-1} upon deuteration of the Schiff base in PR due to H/D exchange (bottom trace). Although the positive band at 1617 cm^{-1} now disappears, the downshift of this band could not be clearly identified (bottom trace). On this basis we assign most of the 1664 and 1630 cm^{-1} bands to the protonated Schiff base stretching vibration in the PR resting state and K intermediate, respectively. A downshift of 34 cm^{-1} from PR to the K intermediate is similar to the shift observed for the BR C═N stretching frequency from BR (1642 cm^{-1}) to K (1609 cm^{-1}) (*33*).

The higher frequency (1664 vs 1642 cm^{-1}) and larger isotope-induced downshift of the protonated Schiff base mode in PR compared to bacteriorhodopsin (*33*) indicates stronger hydrogen bonding of the Schiff base (*35*). The different protein environment in the Schiff base region is also indicated by the higher pK_a of the SB counterion Asp97 in PR compared to the homologous Asp85 in BR (*5*, *6*). Note that a kinetic FTIR study (*5*) utilizing H/D exchange assigned the SB C═N stretching frequency to 1651 cm^{-1}. Resonance Raman measurements led to assignment of the Schiff base C═N vibration as a barely resolvable doublet at 1655/1642 cm^{-1}, although this splitting may arise from a heterogeneous structure near the Schiff base portion of the retinal chromophore (*4*). Reasons for the differences in the various assignments of the Schiff base frequency in PR are not yet known. One factor to further investigate is the existence of a mixture of all-*trans*/13-*cis* chromophores in the light- and dark-adapted forms of PR which could give rise to different Schiff base frequencies.

FTIR Difference Spectra of the Mutant D97N. Residue Asp85 in BR serves as the Schiff base counterion and proton acceptor (*12*, *36*, *37*). Replacement of Asp85 with a neutral residue such as alanine or asparagine causes a red shift of the BR λ_{max} from 570 to near 600 nm, as expected on the basis of a simple point charge model (*38*). Neutralization of Asp97, the homologous residue and Schiff base counterion in the PR, with an asparagine causes a similar red shift from 523 to near 550 nm (Figure 2). A similar effect can be also observed by lowering the pH of wild-type PR due to protonation of Asp97 (*5*, *6*).

FTIR difference spectra of the PR → K transition of D97N (Figure 1, bottom) also reflect the effects of counterion neutralization, since the chromophore C═C stretching mode in the dark state (1540 cm^{-1}) and K photointermediate (1520 cm^{-1}) both downshift approximately 5 cm^{-1}. The downshift of the negative band agrees qualitatively with the observed red shift of the D97N λ_{max} (*26*), and the shift of the positive band indicates that the visible absorption of the K intermediate is almost affected to the same extent. A similar downshift of the C═C stretching mode of the dark state of PR was previously detected by FT Raman (*6*). On the other hand, with a few exceptions discussed below, the WT and D97N PR → K difference spectra are remarkably similar. This includes very similar amide I, chromophore fingerprint, and HOOP mode regions, indicating that both protein structural changes and the chromophore isomerization are not affected appreciably by charge neutralization of the SB counterion.

Most of the changes that are detected in the amide I region between WT and D97N can be attributed to the effects of SB counterion neutralization on the Schiff base vibrations in PR and K. In particular, a decrease in intensity was found for D97N near the negative 1664 cm^{-1} band, consistent with a shift to lower frequency. Furthermore, the positive 1630 cm^{-1} peak downshifts to 1622 cm^{-1}.

Bands near 1597 (+) cm^{-1} and 1413 (−)/1396 (+) cm^{-1} are absent in the D97N mutant. There is also the possibility of the disappearance of an additional band at 1604 (−) cm^{-1}. These frequencies are typical for the antisymmetric and symmetric stretching modes of a carboxylate group, respec-

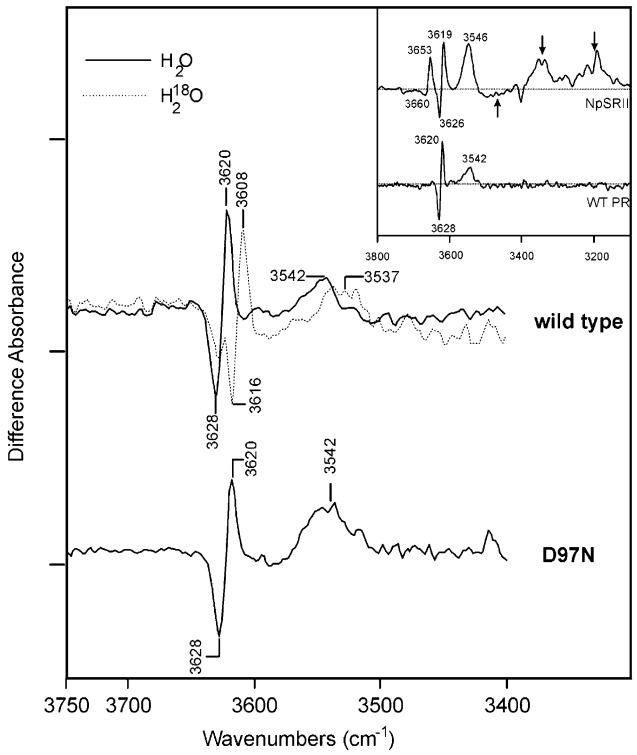

FIGURE 4: Comparison of the wild-type and D97N difference spectra of PR shown in Figure 1 in the 3400−3750 cm^{-1} region: (top) wild-type PR in H_2O (solid line) and $H_2{}^{18}O$ (dotted line); (bottom) the D97N mutant. Spacing of *Y*-axis markers corresponds to 5×10^{-5} OD. Inset: Comparison of the difference spectra of archaeal photoreceptor NpSRII and wild-type PR recorded at 80 K in the 3100−3800 cm^{-1} region. Several broad bands below 3500 cm^{-1} in the NpSRII spectrum, which are marked by arrows, were previously shown to contain contributions from strongly hydrogen-bonded water molecules (*42*).

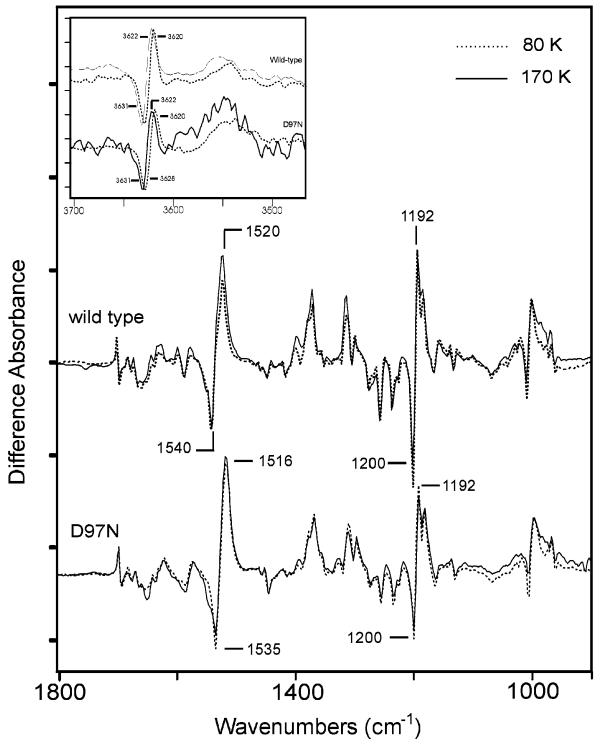

FIGURE 5: Comparison of the wild-type (top) and D97N (bottom) spectra of PR recorded at 80 (solid line) and 170 K (dotted line) in the 900−1800 and 3550−3700 cm^{-1} (inset) regions. Spectra were recorded at 4 cm^{-1} resolution. Spacing of *Y*-axis markers corresponds to 1×10^{-4} OD.

tively (*39*). Thus, it appears on this basis that the Asp97 counterion undergoes a change in its environment during the all-*trans* → 13-*cis* isomerization, possibly reflecting a change in hydrogen bonding due to a repositioning of the protonated Schiff base relative to its counterion.

Identification of Vibrational Bands Due to Internal Water Molecules. Several bands are observed in the 3500−3700 cm^{-1} region in the PR → K difference spectrum (Figure 4, top solid trace). Most prominent is a pair of negative/positive bands appearing at 3628/3620 cm^{-1} and an additional broader positive band near 3542 cm^{-1}. Bands in this region typically arise from the O−H stretching vibrations of weakly hydrogen-bonded protein side-chain hydroxyl groups or internal water molecules. For example, a negative/positive band near 3642/3636 cm^{-1} and two broader positive bands at 3625 and 3570 cm^{-1} were detected in the BR → K transition (*40*) and later photointermediates (*40, 41*). Water bands are also detected in this region of *Neurospora* rhodopsin, an archaeal rhodopsin-like pigment found in *Neurospora crassa*, a filamentous fungus (*17*), and in sensory rhodopsin II from *Natronobacterium pharaonis* (NpSRII) (*42*). In the latter case, several bands appear at a remarkably close frequency to PR, although the higher frequency negative/positive pair at 3660/3653 cm^{-1} is absent in PR (Figure 4, inset). The spectra of NpSRII also exhibit a number of broad bands below 3500 cm^{-1} which might contain contributions from strongly hydrogen-bonded H_2O molecules (see also ref *42*). The PR spectra do not display such prominent bands in this region (Figure 4, inset), although the presence of smaller peaks cannot be excluded.

To unambiguously assign the observed bands to vibrations of internal water molecules, spectra were recorded in $H_2{}^{18}O$. As seen in Figure 4 (top dotted trace), all difference bands in this region downshifted by approximately 12 cm^{-1} due to the ^{16}O → ^{18}O isotope shift, while no spectral changes were observed in the 900−1800 cm^{-1} region (data not shown). A weak negative band remains near 3628 cm^{-1} in the $H_2{}^{18}O$ spectrum, indicating an incomplete exchange with the bulk water. A similar effect was observed in BR even after several days of exposure to $H_2{}^{18}O$ (*40*) and attributed to a very slow exchange rate for internal waters. Note that the residual positive band expected at 3620 cm^{-1} is not observed, most likely due to overlap with the downshifted negative band at 3616 cm^{-1}.

Surprisingly, no spectral changes are observed in this region in the mutant D97N (Figure 4, lower trace). In contrast, the homologous mutation in BR (D85N) results in almost complete disappearance of several assigned water bands for the BR → K (*43*) and BR → L (*44*) difference spectra. On this basis we conclude that, in contrast to BR, the internal water molecules detected by us in PR *are not interacting* closely with the Schiff base counterion Asp97. A similar conclusion was reached by comparing the water bands recorded for the PR → K transition of WT and D97N at 170 K. In this case the spectrum appears to be almost identical except for a small ∼4 cm^{-1} shift of the bands to higher frequency (Figure 5). Our results do not exclude the possibility of strongly hydrogen-bonded water molecules present in the vicinity of Asp97. The O−H stretching vibrations of these molecules would appear below 3500 cm^{-1}, giving rise to broad and poorly resolved bands in the difference spectra,

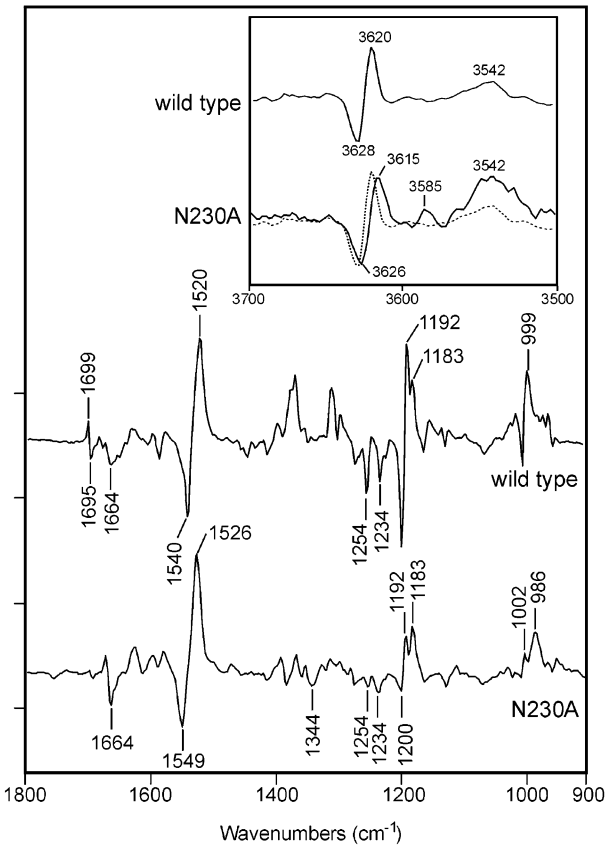

FIGURE 6: Comparison of the wild-type and N230A PR difference spectra recorded at 80 K in the 900−1800 cm^{-1} region. Spectra are recorded at 4 cm^{-1} resolution. Spacing of *Y*-axis markers corresponds to 1×10^{-4} OD. Inset: The same spectra shown in the 3500−3700 cm^{-1} region.

although they might be detected using polarized FTIR spectroscopy (*45*).

FTIR Difference Spectra of the Mutant N230A. Unlike BR, which has a *hydrophobic* residue Ala215 adjacent to Lys216, the group which forms a covalent Schiff base linkage with all-*trans* retinal, PR, has a *polar* residue, Asn230, which is located adjacent to Lys231, the homologous group to Lys216. As discussed below, the polar side chain of Asn230 is in a position to interact with the Schiff base and other groups in the vicinity of the chromophore. Thus, it is possible that Asn230 is perturbed during various steps of the PR photocycle including the primary photoreaction. In fact, a pair of prominent bands appearing at 1699/1695 cm^{-1} (+/−) in the PR → K difference spectrum are possible candidates for C═O stretching vibrations of an Asn or Gln group (*46*). Similar bands at 1707/1701 cm^{-1} (+/−) in the difference spectrum of sensory rhodopsin II were recently assigned to changes in the hydrogen bonding of Asn105 (*16*).

To assign these bands, the PR mutant Asn230 → Ala was produced, which restores the alanine residue present at the analogous position in BR. The visible absorption spectrum of N230A has maximum at 528 nm (Figure 2), a 5 nm red shift from the WT PR. A comparison of the PR → K difference spectra for WT and the mutant N230A is shown in Figure 6. The 1699/1695 cm^{-1} pair of bands clearly disappears in the N230A spectrum. On this basis we assign these bands to perturbations of Asn230 during formation of the K intermediate, possibly due to a change in the hydrogen-bonding strength. A frequency upshift between the negative and positive bands indicates that the hydrogen bond formed by this group is weaker in the light-activated K state.

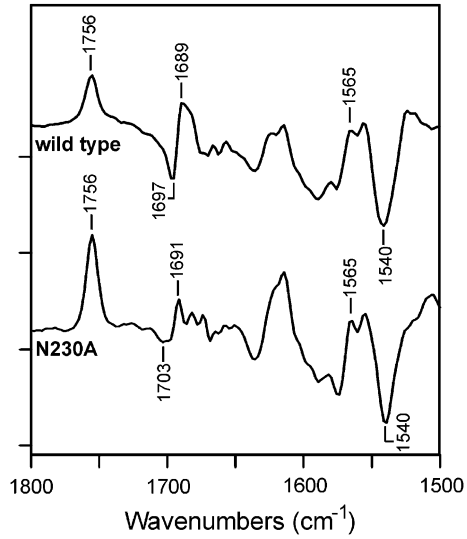

FIGURE 7: Comparison of the wild-type and N230A PR difference spectra recorded at 215 K and 4 cm^{-1} spectral resolution. 3000 scans before and after illumination with yellow (475 nm long pass) light were averaged, and former spectrum was subtracted from the latter.

Several other bands are also affected by the N230A mutation. The ethylenic stretching bands appear at 1549 (−) and 1526 (+) cm^{-1}. The frequency upshift of these bands from the wild-type is opposite to what is expected from the red-shifted absorption maximum of the mutant. One possibility is that under the conditions of experiment some fraction of the protein sample accumulates in a *blue-shifted* dark state possessing the 13-*cis* chromophore. The increase of a negative band near 1344 cm^{-1} associated with the 13-*cis* photocycle in BR (*29*) supports this hypothesis. The presence of a blue-shifted state is not evident from our UV−visible spectra measured at room temperature (Figure 2). However, due to the broadness of this peak, we cannot rule out the presence of such a state. An alternative explanation for the frequency shift is that there exist contributions in this region from other bands such as amide II vibrations of the protein backbone.

Spectral changes in the N230A PR also appear in the O−H stretching region (Figure 6, inset). The 3628/3620 (−/+) cm^{-1} pair of bands in the wild-type spectrum is downshifted to 3626/3615 cm^{-1} in N230A and a small band appears near 3585 cm^{-1} (+). The broad band at 3542 cm^{-1} (+) is present in both spectra. The relatively weak effect of the N230A mutation suggests that the observed water molecules do not interact directly with Asn230 but may be altered as a result of larger protein structural changes caused by the mutation.

In contrast to the wild-type and D97N PR, the N230A spectra recorded at 170 K were different from the 80 K spectra, exhibiting bands typical of the M intermediate. The M intermediate of wild-type PR can be produced only at higher temperature (215 K) by illumination of the protein dark state with yellow light (Figure 7, top). Typical features of the M intermediate are the strong positive band at 1756 cm^{-1} arising from protonation of Asp97 (*6*) and the ethylenic stretching band of the unprotonated chromophore at 1565 cm^{-1} (+), which appears at 1568 cm^{-1} in room temperature time-resolved spectra (*5*). The wild-type spectrum exhibits

strong bands near 1697 (−)/1689 (+) cm^{-1}, which disappear in the N230A mutant, revealing smaller peaks near 1703 and 1691 cm^{-1}. The 1697/1689 cm^{-1} bands are therefore assigned to changes in the Asn230 environment upon the formation of M intermediate. The higher intensity of these peaks compared to the 1699/1695 cm^{-1} pair in the PR → K spectrum (Figure 1) suggests that Asn230 undergoes larger structural changes at this stage of the photocycle.

DISCUSSION

The current study focuses on elucidating the structural changes which occur during the primary photoreaction of proteorhodopsin, a newly discovered retinal-containing integral membrane protein (*2*, *3*). Thus far, no studies of PR have been reported that examine in detail the primary photoreaction, the step which involves the initial storage of the photon energy absorbed by the chromophore and launches subsequent no photon requiring steps in the photocycle. Since the Monterey Bay surface PR studied here is a light-driven proton pump similar to BR [although some recently found variants of this protein may have different function (*1*)], the early photocycle steps and especially the protein structural changes might be expected to be very similar. However, the phylogenetic distance between proteorhodopsin found in γ-proteobacteria and bacteriorhodopsin found in archaebacteria raises the possibility that there exist fundamental differences in the corresponding proton pumping mechanisms.

The results from this study demonstrate that the primary photoevents in BR and PR both involve a similar isomerization of the chromophore from the all-*trans* to 13-*cis* configuration. However, several of our results indicate that structural changes which occur in the photoactive site during this transition are significantly different. These results include the following:

(1) Chromophore structure and isomerization in the initial photoreaction are not affected by neutralization of the SB counterion. The neutralization of Asp97 in PR does not have a strong effect on the initial all-*trans* chromophore structure, its light-induced isomerization to the 13-*cis* form, or the ability to photoreverse it back to the initial state. In addition, the response of protein groups and internal water molecules (see below) is not affected. These findings indicate that the residues in the vicinity of the photoactive site are minimally perturbed by the Asp to Asn substitution.

In contrast, the analogous mutation D85N in BR results in the decrease of the fraction of all-*trans*-retinal isomer (*47*) and has a major effect on the protein structure (*48*). The low-temperature FTIR difference spectra of D85N are also considerably different from the wild type (*44*).

(2) Asn230 participates in initial photoreaction and subsequent structural changes of PR. In contrast to Asp97, substitution of the polar side chain of Asn230 with an alanine has a large effect on the structure of the chromophore, its response to light, thermal stability of the K intermediate, and also the hydrogen bonding of nearby internal water molecules. Indeed, the observed structural changes of Asn230 in the primary photoreaction suggest that this group interacts with the chromophore either directly or via nearby residues. It is also possible that this group forms hydrogen bond(s) with the Schiff base through its side-chain carbonyl group

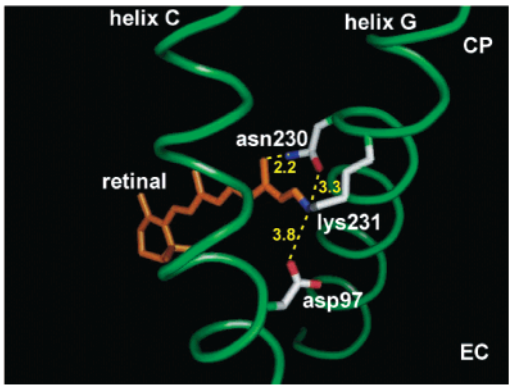

FIGURE 8: Hypothesized positions of Asp97 and Asn230 relative to the Schiff base, which is formed between Lys231 and the retinylidene chromophore. The structure is drawn using the program PyMol (*53*) from the PDB coordinate file 1C3W of the bacteriorhodopsin unphotolyzed state (*49*) with Ala215 (residue homologous to Asn230) replaced by an asparagine. The interatomic distances measured upon the Ala → Asn substitution are based on interactive modeling and provided only to indicate the approximate distance to Asn230. The SB counterion distance is given for bacteriorhodopsin. CP and EC refer to the cytoplasmic and extracellular regions of the protein, respectively.

or alternatively with other protein groups in this region. Although the molecular structure of the active site in PR is not yet known, Asn230 is adjacent to the Schiff base-forming residue Lys231 in an analogous position as Ala215 in bacteriorhodopsin. A replacement of the latter group in the BR active site with an asparagine places this residue within several angstroms from both the SB and the retinal C13 methyl group (Figure 8). The presence of the hydrophilic group of Asn230 may contribute to the differences observed between PR and BR.

(3) No internal water molecules were detected which interact with the SB counterion Asp97. An important feature of the active site in both BR and the sensory receptor, NpSRII, revealed by X-ray crystallographic studies is the presence of two water molecules (W401 and W402) which are in close proximity to the SB counterion (Asp85 and Asp75, respectively) (*49*−*51*). W402 appears to bridge between Asp85, Asp212, and the Schiff base, while W401 has hydrogen bonds formed between the SB counterion and another water molecule on the extracellular side of the protein. In both structures these waters are part of a pentagonal cluster involving the two carboxylate groups (Asp85 and Asp212 in BR and Asp75 and Asp 201 in NpSRII) and an additional water molecule, W406 (*34*, *52*).

The similarity of bands observed in the O−H stretching region of the spectra of wild-type and D97N PR suggests that the water molecules which these bands represent are not associated with Asp97 and located elsewhere in PR. One possible explanation is that there are no water molecules in the immediate vicinity of Asp97, and the Schiff base interacts directly with Asp97. Alternatively, an additional hydrophilic side chain might participate in an interaction involving Asp97 and the SB. One candidate is Asn230, which, as noted above, is located in this region. It is also possible that the water molecules which interact with Asp97 are not strongly perturbed during the early photocycle and therefore do not appear in the PR → K difference spectra.

A clue to the location of the internal water molecules we detect in PR during the primary photoreaction comes from

the similar bands observed in this region in the NpSRII primary photoreaction (Figure 4, inset). The major difference is the appearance of an additional feature in NpSRII consisting of a negative/positive pair of bands at 3660/3653 cm^{-1} (*42*). One explanation for the similarity is that NpSRII and PR share a set of internal water molecules which are not in the immediate vicinity of the SB counterion but are still located close to the pentagonal structure of hydrogen-bonded groups. Alternatively, these internal waters may be located outside the active site. However, they must still interact indirectly with the chromophore or they would not sense the isomerization in the primary photoreaction.

ACKNOWLEDGMENT

We thank Sergey Mamaev and Jerzy Olejnik for helpful discussions and Joel Kralj for assistance during the course of this work.

REFERENCES

1. Wang, W. W., Sineshchekov, O. A., Spudich, E. N., and Spudich, J. L. (2003) Spectroscopic and photochemical characterization of a deep ocean proteorhodopsin, *J. Biol. Chem. 278*, 33985−33991.
2. Béjà, O., Aravind, L., Koonin, E. V., Suzuki, M. T., Hadd, A., Nguyen, L. P., Jovanovich, S. B., Gates, C. M., Feldman, R. A., Spudich, J. L., Spudich, E. N., and DeLong, E. F. (2000) Bacterial rhodopsin: evidence for a new type of phototrophy in the sea, *Science 289*, 1902−1906.
3. Béjà, O., Spudich, E. N., Spudich, J. L., Leclerc, M., and DeLong, E. F. (2001) Proteorhodopsin phototrophy in the ocean, *Nature 411*, 786−789.
4. Krebs, R. A., Dunmire, D., Partha, R., and Braiman, M. S. (2003) Resonance Raman characterization of proteorhodopsin's chromophore environment, *J. Phys. Chem. B 107*, 7877−7883.
5. Friedrich, T., Geibel, S., Kalmbach, R., Chizhov, I., Ataka, K., Heberle, J., Engelhard, M., and Bamberg, E. (2002) Proteorhodopsin is a light-driven proton pump with variable vectoriality, *J. Mol. Biol. 321*, 821−838.
6. Dioumaev, A. K., Brown, L. S., Shih, J., Spudich, E. N., Spudich, J. L., and Lanyi, J. K. (2002) Proton transfers in the photochemical reaction cycle of proteorhodopsin, *Biochemistry 41*, 5348−5358.
7. Alexiev, U., Mollaaghababa, R., Scherrer, P., Khorana, H. G., and Heyn, M. P. (1995) Rapid long-range proton diffusion along the surface of the purple membrane and delayed proton transfer into the bulk, *Proc. Natl. Acad. Sci. U.S.A. 92*, 372−376.
8. Cao, Y., Brown, L. S., Sasaki, J., Maeda, A., Needleman, R., and Lanyi, J. K. (1995) Relationship of proton release at the extracellular surface to deprotonation of the Schiff base in the bacteriorhodopsin photocycle, *Biophys. J. 68*, 1518−1530.
9. Rothschild, K. J., Zagaeski, M., and Cantore, W. A. (1981) Conformational changes of bacteriorhodopsin detected by Fourier transform infrared difference spectroscopy, *Biochem. Biophys. Res. Commun. 103*, 483−489.
10. Bagley, K., Dollinger, G., Eisenstein, L., Singh, A. K., and Zimanyi, L. (1982) Fourier transform infrared difference spectroscopy of bacteriorhodopsin and its photoproducts, *Proc. Natl. Acad. Sci. U.S.A. 79*, 4972−4976.
11. Earnest, T. N., Roepe, P., Braiman, M. S., Gillespie, J., and Rothschild, K. J. (1986) Orientation of the bacteriorhodopsin chromophore probed by polarized Fourier transform infrared difference spectroscopy, *Biochemistry 25*, 7793−7798.
12. Braiman, M. S., Mogi, T., Marti, T., Stern, L. J., Khorana, H. G., and Rothschild, K. J. (1988) Vibrational spectroscopy of bacteriorhodopsin mutants: light-driven proton transport involves protonation changes of aspartic acid residues 85, 96, and 212, *Biochemistry 27*, 8516−8520.
13. Siebert, F. (1990) Resonance Raman and infrared difference spectroscopy of retinal proteins, *Methods Enzymol. 189*, 123−136.
14. Siebert, F., Hein, M., Radu, I., and Engelhard, M. (2002) Time-resolved step-scan FTIR investigations of the photophobic receptor sensory rhodopsin II from *Natronobacterium pharaonis*, *Biophys. J. 82*, 1106.
15. Bergo, V., Spudich, E. N., Scott, K. L., Spudich, J. L., and Rothschild, K. J. (2000) FTIR analysis of the SII540 intermediate of sensory rhodopsin II: Asp73 is the Schiff base proton acceptor, *Biochemistry 39*, 2823−2830.
16. Furutani, Y., Iwamoto, M., Shimono, K., Kamo, N., and Kandori, H. (2002) FTIR Spectroscopy of the M Photointermediate in pharaonis Phoborhodopsin, *Biophys. J. 83*, 3482−3489.
17. Bergo, V., Spudich, E. N., Spudich, J. L., and Rothschild, K. J. (2002) A Fourier transform infrared study of Neurospora rhodopsin: Similarities with archaeal rhodopsins, *Photochem. Photobiol. 76*, 341−349.
18. Brown, L. S., Dioumaev, A. K., Lanyi, J. K., Spudich, E. N., and Spudich, J. L. (2001) Photochemical reaction cycle and proton transfers in Neurospora rhodopsin, *J. Biol. Chem. 276*, 32495−32505.
19. Rothschild, K. J., and Marrero, H. (1982) Infrared evidence that the Schiff base of bacteriorhodopsin is protonated: BR570 and K intermediates, *Proc. Natl. Acad. Sci. U.S.A. 79*, 4045−4049.
20. Siebert, F., and Mäntele, W. (1983) Investigation of the primary photochemistry of bacteriorhodopsin by low-temperature Fourier transform infrared spectroscopy, *Eur. J. Biochem. 130*, 565−573.
21. DeGrip, W. J., and Rothschild, K. J. (2000) in *Molecular Mechanisms in Visual Transduction* (Stravenga, D. G., de Grip, W. J., and Pugh, E. N., Eds.) pp 1−54, Elsevier Science B.V., Amsterdam.
22. Rothschild, K. J., Cantore, W. A., and Marrero, H. (1983) Fourier transform infrared difference spectra of intermediates in rhodopsin bleaching, *Science 219*, 1333−1335.
23. Siebert, F., Mantele, W., and Gerwert, K. (1983) Fourier transform infrared spectroscopy applied to rhodopsin. The problem of the protonation state of the retinylidene Schiff base re-investigated, *Eur. J. Biochem. 136*, 119−127.
24. Kandori, H., Shimono, K., Sudo, Y., Iwamoto, M., Shichida, Y., and Kamo, N. (2001) Structural changes of pharaonis phoborhodopsin upon photoisomerization of the retinal chromophore: infrared spectral comparison with bacteriorhodopsin, *Biochemistry 40*, 9238−9246.
25. Rothschild, K. J., Marrero, H., Braiman, M., and Mathies, R. (1984) Primary photochemistry of bacteriorhodopsin: comparison of Fourier transform infrared difference spectra with resonance Raman spectra, *Photochem. Photobiol. 40*, 675−679.
26. Aton, B., Doukas, A. G., Callender, R. H., Becher, B., and Ebrey, T. G. (1977) Resonance Raman studies of the purple membrane, *Biochemistry 16*, 2995−2999.
27. Bergo, V., Spudich, E. N., Spudich, J. L., and Rothschild, K. J. (2003) Conformational changes detected in a sensory rhodopsin II-transducer complex, *J. Biol. Chem. 278*, 36556−36562.
28. Smith, S. O., Myers, A. B., Mathies, R. A., Pardoen, J. A., Winkel, C., Van den Berg, E. M. M., and Lugtenburg, J. (1985) Vibrational analysis of the all-trans retinal protonated Schiff base, *Biophys. J. 47*, 653−664.
29. Roepe, P. D., Ahl, P. L., Herzfeld, J., Lugtenburg, J., and Rothschild, K. J. (1988) Tyrosine protonation changes in bacteriorhodopsin. A Fourier transform infrared study of bR548 and its primary photoproduct, *J. Biol. Chem. 263*, 5110−5117.
30. Roepe, P., Ahl, P. L., Das Gupta, S. K., Herzfeld, J., and Rothschild, K. J. (1987) Tyrosine and carboxyl protonation changes in the bacteriorhodopsin photocycle. 1. M412 and L550 intermediates, *Biochemistry 26*, 6696−6707.
31. Mathies, R. A., Lin, S. W., Ames, J. B., and Pollard, W. T. (1991) From femtoseconds to biology: Mechanism of bacteriorhodopsin's light-driven proton pump, *Annu. Rev. Biophys. Biophys. Chem. 20*, 491−518.
32. Rothschild, K. J. (1992) FTIR difference spectroscopy of bacteriorhodopsin: Toward a molecular model, *J. Bioenerg. Biomembr. 24*, 147−167.
33. Rothschild, K. J., Roepe, P., Lugtenburg, J., and Pardoen, J. A. (1984) Fourier transform infrared evidence for Schiff base alteration in the first step of the bacteriorhodopsin photocycle, *Biochemistry 23*, 6103−6109.
34. Neutze, R., Pebay-Peyroula, E., Edman, K., Royant, A., Navarro, J., and Landau, E. M. (2002) Bacteriorhodopsin: a high-resolution structural view of vectorial proton transport, *Biochim. Biophys. Acta 1565*, 144−167.

35. Aton, B., Doukas, A. G., Narva, D., Callender, R. H., Dinur, U., and Honig, B. (1980) Resonance Raman studies of the primary photochemical event in visual pigments, *Biophys. J. 29*, 79−94.
36. Otto, H., Marti, T., Holz, M., Mogi, T., Stern, L. J., Engel, F., Khorana, H. G., and Heyn, M. P. (1990) Substitution of amino acids Asp-85, Asp-212, and Arg-82 in bacteriorhodopsin affects the proton release phase of the pump and the pK of the Schiff base, *Proc. Natl. Acad. Sci. U.S.A. 87*, 1018−1022.
37. Fahmy, K., Weidlich, O., Engelhard, M., Tittor, J., Oesterhelt, D., and Siebert, F. (1992) Identification of the proton acceptor of Schiff base deprotonation in bacteriorhodopsin: a Fourier-transform-infrared study of the mutant Asp85→Glu in its natural lipid environment, *Photochem. Photobiol. 56*, 1073−1083.
38. Honig, B., Dinur, U., Nakanishi, K., Balogh-Nair, V., Gawinowicz, M. A., Arnaboldi, M., and Motto, M. G. (1979) An external point-charge model for wavelength regulation in visual pigments, *J. Am. Chem. Soc. 101*, 7084−7086.
39. Barth, A., and Zscherp, C. (2000) Substrate binding and enzyme function investigated by infrared spectroscopy, *FEBS Lett. 477*, 151−156.
40. Fischer, W., Sonar, S., Marti, T., Khorana, H. G., and Rothschild, K. J. (1994) Detection of a water molecule in the active site of bacteriorhodopsin: hydrogen bonding changes during the primary photoreaction, *Biochemistry 33*, 12757−12762.
41. Maeda, A., Sasaki, J., Shichida, Y., and Yoshizawa, T. (1992) Water structural changes in the bacteriorhodopsin photocycle: analysis by Fourier transform infrared spectroscopy, *Biochemistry 31*, 462−467.
42. Kandori, H., Furutani, Y., Shimono, K., Shichida, Y., and Kamo, N. (2001) Internal water molecules of pharaonis phoborhodopsin studied by low-temperature infrared spectroscopy, *Biochemistry 40*, 15693−15698.
43. Shibata, M., Tanimoto, T., and Kandori, H. (2003) Water molecules in the Schiff base region of bacteriorhodopsin, *J. Am. Chem. Soc. 125*, 13312−13313.
44. Maeda, A., Sasaki, J., Yamazaki, Y., Needleman, R., and Lanyi, J. K. (1994) Interaction of aspartate-85 with a water molecule and the protonated Schiff base in the L intermediate of bacteriorhodopsin: a Fourier-transform infrared spectroscopic study, *Biochemistry 33*, 1713−1717.
45. Kandori, H., and Shichida, Y. (2000) Direct observation of the bridged water stretching vibrations inside a protein, *J. Am. Chem. Soc. 122*, 11745−11746.
46. Barth, A. (2000) The infrared absorption of amino acid side chains, *Prog. Biophys. Mol. Biol. 74*, 141−173.
47. Song, L., Yang, D. F., Elsayed, M. A., and Lanyi, J. K. (1995) Retinal isomer composition in some bacteriorhodopsin mutants under light and dark-adaptation conditions, *J. Phys. Chem. 99*, 10052−10055.
48. Brown, L. S., Kamikubo, H., Zimanyi, L., Kataoka, M., Tokunaga, F., Verdegem, P., Lugtenburg, J., and Lanyi, J. K. (1997) A local electrostatic change is the cause of the large-scale protein conformation shift in bacteriorhodopsin, *Proc. Natl. Acad. Sci. U.S.A. 94*, 5040−5044.
49. Luecke, H., Schobert, B., Richter, H. T., Cartailler, J. P., and Lanyi, J. K. (1999) Structure of bacteriorhodopsin at 1.55 Å resolution, *J. Mol. Biol. 291*, 899−911.
50. Luecke, H., Schobert, B., Lanyi, J. K., Spudich, E. N., and Spudich, J. L. (2001) Crystal structure of sensory rhodopsin II at 2.4 angstroms: insights into color tuning and transducer interaction, *Science 293*, 1499−1503.
51. Royant, A., Nollert, P., Edman, K., Neutze, R., Landau, E. M., Pebay-Peyroula, E., and Navarro, J. (2001) X-ray structure of sensory rhodopsin II at 2.1 Å resolution, *Proc. Natl. Acad. Sci. U.S.A. 98*, 10131−10136.
52. Pebay-Peyroula, E., Royant, A., Landau, E. M., and Navarro, J. (2002) Structural basis for sensory rhodopsin function, *Biochim. Biophys. Acta 1565*, 196−205.
53. DeLano, W. L. (2003) DeLano Scientific LLC, South San Francisco, CA 94080.
54. Man, D., Wang, W., Sabehi, G., Aravind, L., Post, A. F., Massana, R., Spudich, E. N., Spudich, J. L., and Béjà, O. (2003) Diversification and spectral tuning in marine proteorhodopsins, *EMBO J. 8* 1725−1731.

BI0361968